Cancer Research

Receptor Activator of NF-κB Ligand Enhances Breast Cancer–Induced Osteolytic Lesions through Upregulation of Extracellular Matrix Metalloproteinase Inducer/CD147

Nadia Rucci[1], Danilo Millimaggi[2], Marianna Mari[2], Andrea Del Fattore[1], Mauro Bologna[1], Anna Teti[1], Adriano Angelucci[1], and Vincenza Dolo[2]

Abstract

Breast cancer shows a strong predilection to metastasize to bone. Cell surface glycoprotein extracellular matrix metalloproteinase inducer (EMMPRIN)/CD147 induces metalloproteinases (MMP) and vascular endothelial growth factor (VEGF), which may support osteoclastic activity and increased incidence of breast cancer bone metastases. In support of this hypothesis, we observed that MDA-MB-231 human breast tumor cells engineered to overexpress EMMPRIN strongly induced osteolytic lesions in immunodeficient mice, which was blunted by *in vivo* treatment with an EMMPRIN blocking antibody. Similarly, these cells exhibited increased expression of MMP-9 and VEGF relative to control cells. Treatment of MDA-MB-231 cells with the osteoclastogenic cytokine receptor activator of NF-κB ligand (RANKL) upregulated EMMPRIN expression with a parallel increase of MMP-9 and VEGF. Conditioned medium from osteoblasts similarly increased EMMPRIN, MMP-9, and VEGF expression in cells. Osteoblast treatment with the RANKL decoy receptor osteoprotegerin abolished this effect. EMMPRIN overexpression stimulated MDA-MB-231 cell invasion but not proliferation. Conversely, small interfering RNA–mediated knockdown of EMMPRIN downregulated MMP-9 and VEGF basal expression and RANKL-stimulated expression, and reduced cell invasion. Our results argue that EMMPRIN drives breast cancer–induced osteolytic lesions and that activation of the RANKL pathway increases EMMPRIN in osteotropic tumor cells, in turn enhancing tumor-induced bone resorption. *Cancer Res; 70(15); 6150–60.* ©*2010 AACR.*

Introduction

Extracellular matrix metalloproteinase inducer (EMMPRIN), also known as CD147, basigin, M6, and tumor cell–derived collagenase stimulating factor, is a 58-kDa transmembrane glycoprotein belonging to the immunoglobulin superfamily (1, 2). It is expressed in normal tissues such as epidermis, retinal pigment epithelium, breast lobules, and ductules, suggesting a physiologic role in tissue remodeling by inducing stromal metalloproteinases (MMP; refs. 3–5). Several data have clearly shown a key role for EMMPRIN in tumor progression and metastasis. Indeed, high levels of EMMPRIN were reported in many tumors, including breast cancer, lymphoma, oral squamous cell carcinoma, glioma, melanoma, lung, bladder, and kidney carcinomas (6). Accordingly, EMMPRIN expression has been associated with known risk factors for breast cancer and with poor prognosis of breast cancer patients (7).

Authors' Affiliations: Departments of [1]Experimental Medicine and [2]Health Sciences, University of L'Aquila, L'Aquila, Italy

Corresponding Author: Adriano Angelucci, University of L'Aquila, Department of Experimental Medicine, Via Vetoio-Coppito 2, 67100 L'Aquila, Italy. Phone: 39-0862-433549; Fax: 39-0862-433523; E-mail: adriano.angelucci@univaq.it.

doi: 10.1158/0008-5472.CAN-09-2758

The action of EMMPRIN in tumor progression was initially linked to the stimulation of several MMPs in fibroblasts surrounding the tumor (6, 8, 9). However, EMMPRIN is also able to induce MMP production in tumor cells in an autocrine fashion (10) and to enhance *in vivo* tumor angiogenesis by upregulating vascular endothelial growth factor (VEGF; refs. 11, 12).

Breast carcinoma, along with multiple myeloma, prostate, lung, and thyroid carcinomas, are prone to metastasize to bone (13, 14). Indeed, 70% of patients who die for breast cancer is found to have skeletal lesions at autopsy (13, 14). Once bone metastases have been established, the chance of survival as well as the quality of life dramatically drop, with a clinical outcome characterized by intractable pain, nerve compression syndromes, increased risk of fractures, and hypercalcaemia (15). Overt breast bone metastases are generally osteolytic in nature and rely on the ability of tumor cells to activate osteoclast bone resorption, which is a pivotal event in the disruption of bone and in the creation of physical space into which the tumor intrudes (16–18).

Based on the well-known role of EMMPRIN in tumor development, the aim of the present study was to test the potential involvement of this molecule in the ability of breast cancer cells to induce osteolytic lesions in bone. Our findings revealed that the human breast cancer cell line, MDA-MB-231 (MDA-231) overexpressing EMMPRIN, injected into the tibias of immunodeficient mice, had a

greater ability to induce the development of radiographically detectable osteolytic lesions. Conversely, *in vivo* treatment with an EMMPRIN blocking antibody reduced the onset of the osteolytic lesions as well as the tumor burden. Moreover, our data showed that the expression of EMMPRIN is enhanced by a mechanism that involves the activation of the receptor activator of NF-κB ligand (RANKL) pathway, pivotal for the control of bone resorption.

Materials and Methods

Materials

DMEM, fetal bovine serum (FBS), penicillin, streptomycin, and trypsin were from Invitrogen. Sterile plastic ware was purchased from Becton Dickinson and Costar. Trizol reagent, reverse transcription-PCR (RT-PCR) primers and reagents, lipofectamine, oligofectamine, opti-MEM, and PLUS reagent were from Invitrogen. The Brilliant SYBR Green QPCR master mix was from Stratagene. The enhanced chemiluminescence (ECL) kit and Hybond nitrocellulose were from Amersham Pharmacia Biotech. Matrigel was purchased from BD Biosciences. Anti-VEGF antibody (#MAB293) was purchased from R&D Systems, Inc. Anti-EMMPRIN antibody (#sc-53582), goat anti-rabbit IgG horseradish peroxidase (HRP)–conjugated antibody (#sc-2004), small interfering RNA (siRNA) duplexes specific for human EMMPRIN/CD147 (#sc-35298), and siRNA transfection reagent (#sc-29528) were from Santa Cruz Biotechnology, Inc. The UM-8D6 clone of EMMPRIN blocking antibody was purchased from Ancell. All other reagents were obtained from Sigma Aldrich Co.

Cell lines

The human breast cancer cell line MDA-MB-231 (MDA-231) was purchased from the American Tissue Culture Collection (ATCC) and used within 3 months after receipt or resuscitation of frozen aliquots. The authentication of the cell line was assured by the provider through the realization of cytogenetic analysis (that can be consulted at http://www.atcc.org). Cells were cultured in DMEM supplemented with 10% FBS, 100 IU/mL penicillin, 100 μg/mL streptomycin, and 2 mmol/L L-glutamine, and according to ATCC suggestion.

Isolation of human umbilical vein endothelial cells

Human umbilical vascular endothelial cells (HUVEC) were isolated from umbilical cords as previously described (19) and were grown on 1% gelatin-coated flasks in DMEM supplemented with 10% FBS, 10% newborn calf serum, 20 mmol/L HEPES, 6 U/mL heparin, 2 mmol/L glutamine, 50 mg/mL endothelial cell growth factor, 100 IU/mL penicillin, and 100 μg/mL streptomycin. Routine characterization of HUVEC cells included cell viability assessment and morphologic observation. Cells were used from the third to fifth passages of culture.

Cell transfection

The MDA-231 cell line was transfected with the pcDNA3 plasmid containing the entire *EMMPRIN* sequence fused to the COOH terminus of green fluorescent protein (GFP; MDA-231-EMMPRIN; ref. 20) using lipofectamine and PLUS reagent. For intratibial injection experiments, we used EMMPRIN stably transfected MDA-231 cells by selecting G418-resistant clones, which were screened by GFP fluorescence detection using a microscope. Positive clones were pooled to minimize clonal variations. Control transfectants were generated by transfection of MDA-231 cells with empty pcDNA3 vector (MDA-231-empty).

Conditioned media

MDA-231-empty and MDA-231-EMMPRIN cells were allowed to grow in DMEM plus 10% FBS until 80% confluence. Primary osteoblast cultures were obtained from the calvariae of 7-day-old CD1 mice as previously described (21). These cells expressed the osteoblast markers alkaline phosphatase, runt-related transcription factor 2, parathyroid hormone/parathyroid hormone–related peptide receptor, and type I collagen and osteocalcin. At the first passage, cells were grown in DMEM plus 10% FBS until 80% confluence. The media were then replaced with serum-free media, and after 48 hours, supernatants were collected, centrifuged, and stored at −80°C until use. For the experiments of RANKL inhibition, primary osteoblasts were treated with 100 ng/mL osteoprotegerin (OPG) or with vehicle (PBS), then after 48 hours, supernatants were collected, centrifuged, and stored at −80°C until use.

Treatment with siRNA

MDA-231 cells were trypsinized and plated in 3.5-cm culture dishes. At ~50% confluence, cells were transfected with the annealed siRNA-EMMPRIN or with scramble siRNA as negative control of gene silencing (final concentration, 100 nmol/L), using the siRNA transfection reagent (Santa Cruz). Cells were cultured with siRNAs for 48 hours.

Real-time RT-PCR

Total RNA was extracted using the Trizol procedure. First-strand cDNA was synthesized from 2 μg RNA using Moloney murine leukemia virus reverse transcriptase. The resulting cDNA (0.1 μg) was subjected to PCR amplification. Real-time PCRs were performed using the Brilliant SYBR Green QPCR master mix with the following primer pairs: glyceraldehyde-3-phosphate dehydrogenase (GAPDH; Fw: 5′-CTGCACCACCAACTGCTTAG-3′; Rv: 5′-AGGGAGGGGAGCCGGCTGTC-3′), EMMPRIN (Fw: 5′-GACGACCAGTGGGGAGAGTA-3′; Rv: 5′-GCGAGGAACTCACGAAGAAC-3′), MMP-9 (Fw: 5′-TGAATCAGCTGGCTTTTGTG-3′; Rv: 5′-GTGGATAGCTCGGTGGTGTT-3′), and VEGF (Fw: 5′-CTACCTCCACCATGCCAAGT-3′; Rv: 5′-TGGTGATGTTGGACTCCTCA-3′).

For all real-time PCRs, the conditions were as follows: 40 cycles, 94°C for 25 seconds, 60°C for 25 seconds, and 72°C for 25 seconds.

Western blotting

For protein extraction, cells were lysed in radioimmunoprecipitation assay buffer [50 mmol/L Tris-HCl (pH 7.5), 150 mmol/L NaCl, 1% Nonidet P-40, 0.5% sodium

deoxycholate, 0.1% SDS] containing protease inhibitors. Proteins were resolved by 10% SDS-PAGE and transferred to nitrocellulose membranes. Blots were probed with the primary antibody for 1 hour at room temperature, were washed, and were incubated with the appropriate HRP-conjugated secondary antibodies for 1 hour at room temperature. Protein bands were revealed by ECL detection.

Cord formation assay

HUVECs were starved overnight in MEDIUM199 with 1% FBS. Wells (48-well plates) were coated with 150 μL Matrigel at 4°C and incubated for 30 minutes at 37°C. Cells (15,000/well) were plated onto the Matrigel-coated wells and incubated with MEDIUM199 containing 2 μg/mL heparin and 30% conditioned medium from MDA-231 cells treated as follows: MDA-231 cells transfected with siRNA-EMMPRIN or with scramble siRNA and treated with vehicle (PBS) or 30 ng/mL RANKL. After 18 hours, the experiment was stopped and the cells were photographed under phase-contrast microscopy. Average numbers of branching points formed in the cultures were counted from triplicate wells.

Flow cytometry analysis

Confluent MDA-231-empty and MDA-231-EMMPRIN cells were detached, collected, and incubated with 10 μg/mL of anti-EMMPRIN antibody for 1 hour at 4°C. Cells were subsequently washed in PBS and incubated with FITC-labeled secondary antibody for 1 hour at 4°C. After washing in PBS, cell surface immunofluorescence was analyzed by a flow cytometer fluorescence-activated cell sorting (FACS) scan (Becton Dickinson).

Intratibial injection of tumor cells

Four-week-old female immunodeficient BALB/c-*nu/nu* mice (Charles River) were maintained under sterile conditions. All experimental procedures involving animals and their care were approved by our Institutional Review Board and complied with national and international laws and policies (EEC Council Directive 86/609, OJ L 358, 1, Dec. 12, 1987; Italian Legislative Decree 116/92, *Gazzetta Ufficiale della Repubblica Italiana* n. 40, Feb. 18, 1992; NIH guide for the Care and Use of Laboratory Animals, NIH Publication no. 85-23, 1985). Mice were anaesthetized with i.p. injection of pentobarbital (60 mg/kg). A syringe with a 26 1/2 G needle was subsequently inserted in the proximal end of the tibia, and tumor cells (1×10^4/10 μL PBS) were injected into the intramedullary space (22, 23). Radiographs were taken at 26, 34, and 42 days after injection.

For the *in vivo* treatment with the EMMPRIN blocking antibody, we followed the protocol described by Damsker and colleagues (24). Briefly, mice were subjected to intratibial injection with MDA-231 cells as described above. Starting the day after the injection, animals received i.p. vehicle (PBS), 5 μg of EMMPRIN blocking antibody (clone UM-8D6, Ancell), or IgG1 from control immune serum. Treatments were repeated twice weekly until the end of the experiment.

Assessment of osteolytic lesions

Mice were anesthesized and subjected to X-ray analysis (36 KPV for 10 s) using a Cabinet X-ray system (Faxitron model n.43855A). Osteolytic lesions were identified on radiographs as radio-opaque regions, and their incidence was expressed as percent of tibiae that developed osteolytic lesions versus the total number of tibiae injected with tumor cells. Radiographs were then scanned using the Bio-Rad GS800 scanning densitometer, and quantification of the osteolytic area per tibia was performed using the Bio-Rad Quantity One image analysis software. For histologic examination, tibiae were dissected, cleaned from soft tissues, and fixed in 4% formaldehyde in 0.1 mol/L phosphate buffer (pH 7.2). Samples were then decalcified in EDTA and embedded in paraffin. Sections were cut and stained with H&E to evaluate the displacement of bone marrow by tumor cells as well as the tumor diameter. Sections were also stained for the typical osteoclast marker tartrate-resistant acid phosphatase and were subjected to histomorphometric analysis.

Cell proliferation assay

MDA-231 cells were cultured in 96-well plates and allowed to proliferate until subconfluence for 72 hours. Cell proliferation was assessed by the 2,3-bis[2-methoxy-4-nitro-5-sulfophenyl]-2H-tetrazolium-5-carboxanilide inner salt (XTT) Cell Proliferation Assay (Sigma Aldrich Co.). This method measures the reduction of a tetrazolium component (XTT) into the soluble formazan product by the mitochondria of viable cells. Using a microplate reader, the absorbance of the samples was measured at a wavelength of 450 nm.

Migration and invasion assays

Migration was performed by the modified Boyden chamber method (25). HUVECs were seeded on 12-μm polycarbonate filters coated with 4.5 $\mu g/cm^2$ gelatin in the upper compartment of the Transwell chambers and were allowed to migrate for 6 hours. Conditioned media from parental MDA-231 cells, MDA-231-empty, and MDA-231-EMMPRIN cells were used as chemoattractants. Filters were then stained with H&E, and cell migration ability was evaluated by counting cells migrated to the lower side of the filters in five randomly chosen fields/filter. Invasion assays with MDA-231 transfectants were performed in a similar manner except that the filters were coated with reconstituted Matrigel (35 $\mu g/cm^2$) and NIH3T3 conditioned medium was used as chemoattractant.

Protease expression by zymography

Expression and activation of pro–MMP-9 (gelatinase B) in MDA-231 conditioned media were analyzed by zymography. This assay was performed using 10% SDS-polyacrylamide gel copolymerized with 0.1 mg/mL gelatin. Gels were washed three times with 50 mmol/L Tris-HCl (pH 7.4) containing 2% Triton X-100 for 15 minutes under agitation to remove SDS, then they were incubated with Tris-HCl (pH 7.4) plus 10 mmol/L $CaCl_2$ and 200 mmol/L NaCl for 24 hours at 37°C. At the end of incubation, gels were fixed and stained with 0.1% Coomassie blue solution. Gelatinase activity was

visualized as white bands on a blue background, which indicated proteolysis of the substrate.

Data analysis

In vitro and *in vivo* experiments were repeated at least three and two times, respectively. Results are expressed as the mean ± SEM or as mean ± SD for the histomorphometric analysis and for the determination of tumor area. Statistical analysis was performed by one-way ANOVA, followed by the unpaired Student's *t* test. A *P* value of <0.05 was deemed to be significant.

Results

Characterization of MDA-231 breast cancer cells with modulated EMMPRIN expression

Compared with MDA-231 empty vector–transfected cells, transient transfection of MDA-231 cells with the EMMPRIN vector resulted in a 10-fold increase of EMMPRIN mRNA (Fig. 1A), which was paralleled by an increase of cell surface EMMPRIN as assessed by FACS analysis (Fig. 1A, inset). EMMPRIN overexpression was accompanied by a significant increase of MMP-9 mRNA expression (Fig. 1B) and activity (Fig. 1B, inset). In addition, the expression of both VEGF mRNA (Fig. 1C) and protein (Fig. 1C, inset) was significantly increased in MDA-231-EMMPRIN cells.

Consistent with the induction of pro–MMP-9 activity, EMMPRIN overexpression resulted in a higher *in vitro* invasiveness of MDA-231 cells (Fig. 1D), whereas cell proliferation was not affected (Fig. 1E). Moreover, the conditioned medium from MDA-231-EMMPRIN cells stimulated the migration of the HUVECs relative to cells incubated with conditioned medium from parental MDA-231 cells or from MDA-231-empty cells (Fig. 1F). This effect is consistent with the increased expression of VEGF induced by EMMPRIN shown in Fig. 1C.

EMMPRIN knockdown by siRNA in MDA-231 cells inhibited EMMPRIN mRNA expression by 80% (Fig. 2A). This was paralleled by a significant reduction of EMMPRIN at the protein level (Fig. 2A, inset), as well as of the downstream target genes MMP-9 (Fig. 2B) and VEGF (Fig. 2C). Reliably, also MMP-9 activity (Fig. 2B, inset), VEGF protein expression (Fig. 2C, inset), and MDA-231 invasion (Fig. 2D) were impaired by EMMPRIN knockdown.

Effect of EMMPRIN on the incidence of osteolytic lesions

MDA-231 cells used in our experiments were highly osteotropic, and when injected into the bone of immunodeficient mice, they grew causing osteolytic lesions that increased over time in a progressive fashion (Fig. 3A). We therefore sought to investigate whether modulation of EMMPRIN expression resulted in an altered ability of MDA-231 cells to induce radiographically detectable osteolytic lesions *in vivo*. To this aim, we compared the effects of MDA-231-empty vector cells and MDA-231-EMMPRIN cells after their inoculation into the tibiae of nude mice. The incidence of osteolytic lesions was significantly higher in mice receiving MDA-231-EMMPRIN cells versus those receiving MDA-231-empty vector cells (Fig. 3A, graph). The extension of osteolytic areas instead was not affected by the level of EMMPRIN expression (Fig. 3B).

In vivo effect of EMMPRIN blocking

We next sought to address whether EMMPRIN inhibition could exert any effect on *in vivo* tumor growth to bone. To this aim, mice intratibially inoculated with MDA-231 cells were treated with an EMMPRIN blocking antibody, twice weekly until the end of the experiment (24). Results evidenced the ability of the blocking antibody to reduce the incidence of osteolytic lesions, relative to mice treated with vehicle or with control immune serum (IgG; Fig. 3C). Densitometric analysis of the X-ray–detected osteolytic lesions (Fig. 3Da) evidenced a trend of decrease of the osteolytic area in the anti-EMMPRIN–treated group (Fig. 3E, right columns), whereas tumor area, evaluated in tibia sections stained with H&E (Fig. 3Db), was significantly reduced (Fig. 3E, left columns). Interestingly, histomorphometric analysis performed on tibia sections stained with H&E (Fig. 3Dc) or for the osteoclast marker tartrate-resistant acid phosphatase (data not shown) evidenced a significant reduction of osteoclast surface (Oc.S/BS) as well as osteoclast number (Oc.N/BS) in mice treated with the EMMPRIN blocking antibody versus vehicle- or IgG-treated mice (Fig. 3Dd). Detection of vascularization by immunohistochemistry for the von Willebrand factor showed no differences among the three groups (data not shown).

Effect of RANKL on EMMPRIN expression

To address the mechanism underlying the ability of EMMPRIN to influence the incidence of osteolytic lesions, parental MDA-231 cells were exposed to conditioned medium from osteoblasts (OBsCM), which are known to produce paracrine effectors of breast cancer growth into the bone. Interestingly, OBsCM induced an increase in EMMPRIN, MMP-9, and VEGF expression in MDA-231 cells versus cells treated with the control medium (Fig. 4A). We next asked which factor produced by osteoblasts could modulate EMMPRIN expression in breast cancer cells. We focused on RANKL, which is considered a key inducer of osteolytic bone metastasis through its pro-osteoclastogenic activity. To address this aspect, osteoblasts were treated with OPG, a decoy receptor that physiologically inhibits RANKL activity. In this circumstance, OPG reduced the increase of EMMPRIN mRNA induced by OBsCM. Similar results were observed also for the downstream genes *MMP-9* and *VEGF* (Fig. 4A).

To confirm the specific role of RANKL in modulating EMMPRIN and its downstream genes, MDA-231 cells were treated with RANKL, which resulted in a time-dependent increase in EMMPRIN expression both at the mRNA (Fig. 4B) and the protein level (Fig. 4B, inset). Consistently, RANKL increased the expression of the EMMPRIN downstream genes, *MMP-9* (Fig. 4C) and *VEGF* (Fig. 4D). A parallel increase of MMP-9 activity (Fig. 4C, inset) and VEGF protein expression (Fig. 4D, inset) was seen after 16 hours of treatment with RANKL. Notably, the effect of RANKL on MMP-9 and VEGF

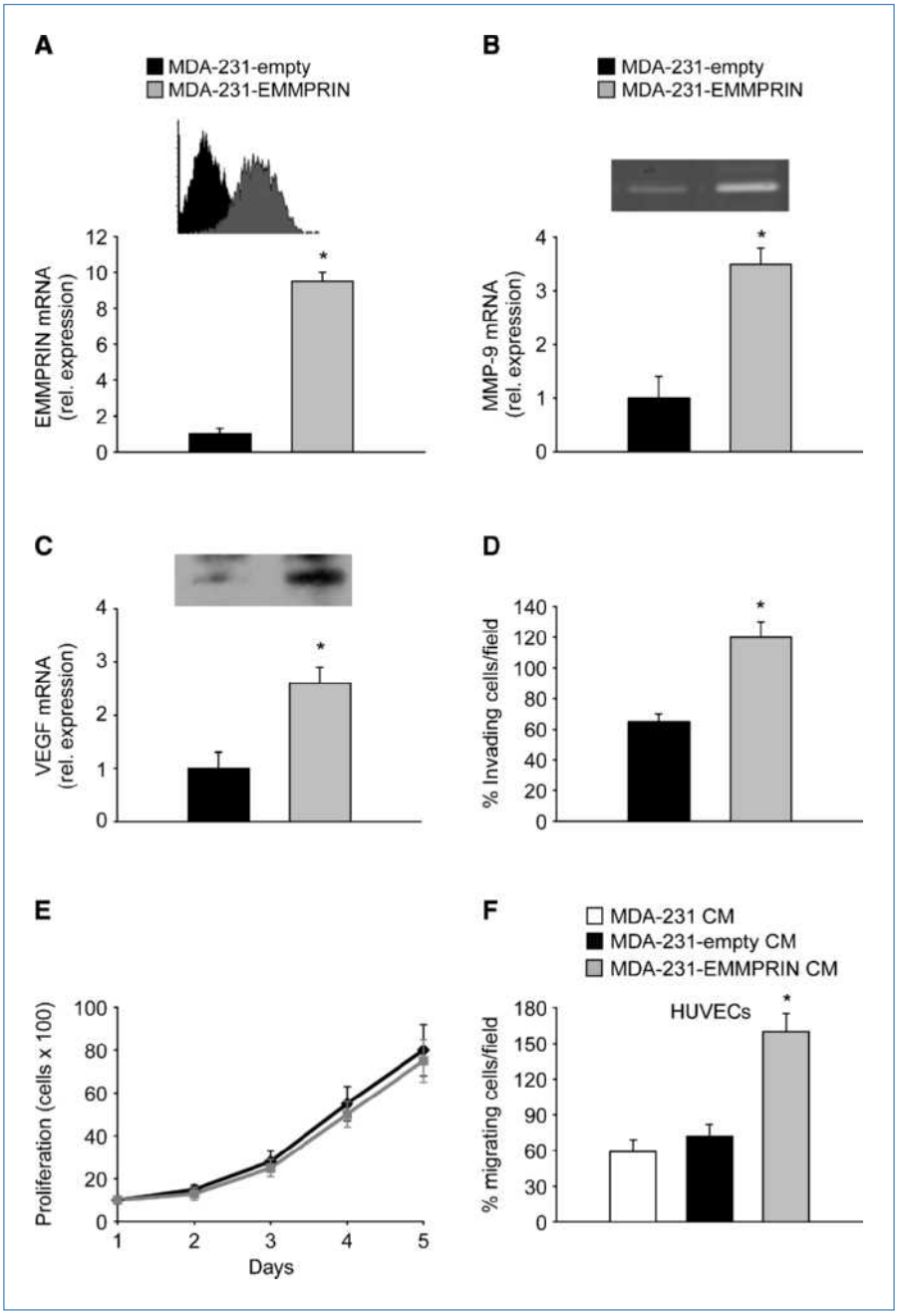

Figure 1. Effect of EMMPRIN overexpression on MDA-231 cells. A to E, the human breast cancer cell line MDA-MB-231 (MDA-231) was stably transfected with a construct carrying the EMMPRIN gene (MDA-231-EMMPRIN) or with an empty vector (MDA-231-empty) as control. Cells were cultured in DMEM plus 10% FBS. A to C, cells were collected at confluence and RNA was extracted and reverse transcribed. The resulting cDNA was subjected to comparative real-time PCR using primer pairs and conditions specific for (A) EMMPRIN, (B) MMP-9, and (C) VEGF. Data are normalized versus the housekeeping gene GAPDH. Columns, mean of three independent experiments; bars, SEM; *, $P < 0.05$ versus MDA-231-empty. Inset, (A) EMMPRIN membrane surface expression detected by FACS analysis (gray profile), (B) MMP-9 activity by zymography in conditioned media from MDA-231-empty and MDA-231-EMMPRIN cells, and (C) VEGF protein expression by Western blot. Pictures are representative of three experiments with similar results. D, invasion assay. Cells were trypsinized and plated in Transwells onto 12-μm pore membrane precoated with Matrigel. After 8 h, the number of cells invading the Matrigel substrate was assessed as described in Materials and Methods. Columns, mean of three independent experiments; bars, SEM; *, $P < 0.05$ versus MDA-231-empty. E, proliferation assay. Cells were cultured in 96-well cell culture plates for 72 h, then proliferation was assessed by the XTT cell proliferation assay (black line, MDA-231-empty; gray line, MDA-231-EMMPRIN). F, migration assay. HUVECs were cultured onto filters coated with gelatin in the upper compartment of the Transwell chambers and were allowed to migrate using as chemoattractants conditioned media from MDA-231 cells (MDA-231-CM), MDA-231 cells transfected with empty vector (MDA-231-empty) and MDA-231 cells overexpressing EMMPRIN (MDA-231-EMMPRIN). Six hours after plating, cells that had migrated were evaluated as described in Materials and Methods. Columns, mean of three independent experiments; bars, SEM; *, $P < 0.05$ versus MDA-231-empty.

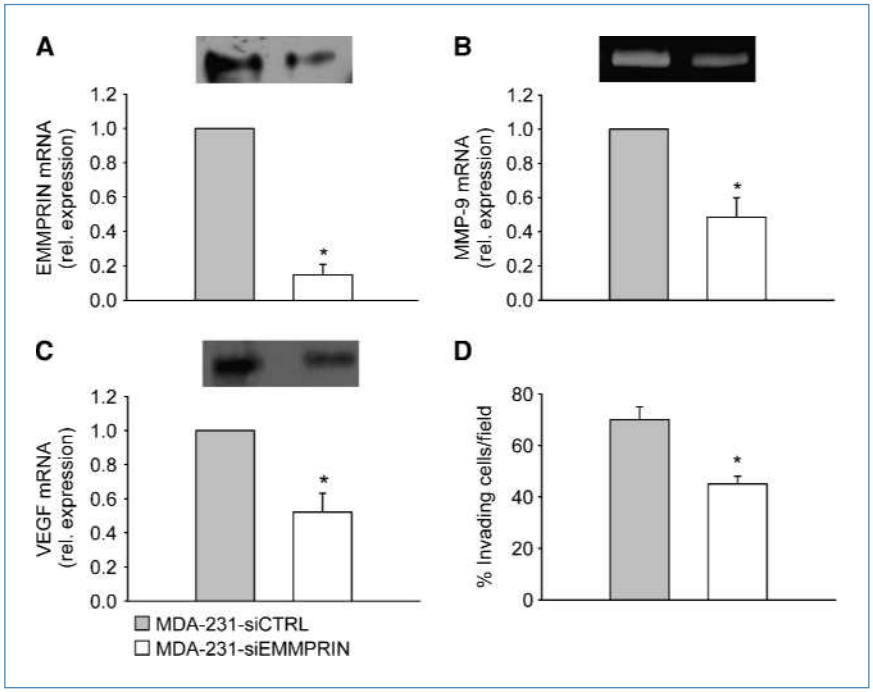

Figure 2. Knockdown of EMMPRIN by siRNA. MDA-231 cells were treated with EMMPRIN-specific siRNA (MDA-231-siEMMPRIN) or scramble siRNA (MDA-231-siCTRL) as control. A to C, cells were collected, the RNA was extracted, and were reverse transcribed. The resulting cDNAs was subjected to comparative real-time PCR using primer pairs and conditions specific for (A) EMMPRIN, (B) MMP-9, and (C) VEGF. Data are normalized versus the housekeeping gene GAPDH. Columns, mean of three independent experiments; bars, SEM; *, $P < 0.05$ versus MDA-231-siCTRL. Inset, the protein expression of (A) EMMPRIN, (B) MMP-9 activity of conditioned media from MDA-231-siCTRL and MDA-231-siEMMPRIN, and (C) VEGF protein expression. Pictures are representative of three experiments with similar results. D, invasion assay. Cells were trypsinized and plated in Transwells onto a 12-μm pore membrane precoated with Matrigel. After 8 h, the number of cells invading the Matrigel substrate was evaluated as described in Materials and Methods. Columns, mean of three independent experiments; bars, SEM; *, $P < 0.05$ versus MDA-231-siCTRL.

expression was indeed EMMPRIN dependent because in MDA-231 cells in which EMMPRIN was silenced by siRNA (Fig. 5A), treatment with RANKL failed to increase both MMP-9 (Fig. 5B) and VEGF (Fig. 5C) mRNAs.

We next evaluated the cellular effect on HUVECs of conditioned medium from MDA-231 cells silenced for EMMPRIN. Conditioned medium from MDA-231-siCTRL cells was able to stimulate in HUVEC cultures the formation of well-organized cord-like structures, and this effect was more evident if MDA-231-siCTRL cells were treated with RANKL (Fig. 5D). In contrast, conditioned medium from MDA-231 cells silenced for EMMPRIN (MDA-231-siEMMPRIN) showed a reduced capacity to stimulate cord formation, and this effect was not affected by the treatment of MDA-231-siEMMPRIN with RANKL (Fig. 5D).

Discussion

EMMPRIN is a transmembrane glycoprotein overexpressed in many carcinomas compared with benign and normal tissues (26–29). Indeed, several pathophysiologic roles of this MMP inducer have been identified, including the promotion of tumorigenicity, invasion, and metastasis (20); enhancement of tumor angiogenesis (11); resistance to anoikis (30); and chemoresistance (31, 32). In the present study, we showed that EMMPRIN is a gene downstream of RANKL, which enhances the ability of osteotropic breast cancer cells to induce osteolytic tumors. This observation can be relevant for therapy, considering that a fully humanized RANKL-neutralizing antibody, denosumab, is in clinical trials for bone metastatic diseases. In addition, an anti-EMMPRIN antibody is currently being evaluated in preclinical studies as a potential therapeutic agent in head and neck cancers (33).

With the aim of characterizing EMMPRIN in the osteotropic human breast cancer cell line MDA-231, we observed that overexpression of EMMPRIN induced MMP-9 mRNA and activity, together with an increased *in vitro* invasiveness. Conversely, knockdown of EMMPRIN by specific siRNA reduced MMP-9 activity and impaired cell invasion. Our current data are in keeping with the known functions of EMMPRIN in human malignancies and strengthen the key role played by this molecule in tumor progression. In contrast, we did not observe any modulation of *in vitro* proliferation. Indeed, this result agrees with the data from Marieb and colleagues (34) showing that increased EMMPRIN expression stimulated anchorage-independent but not anchorage-dependent growth of breast cancer cells.

In this study, EMMPRIN was found to enhance VEGF gene and protein expression in our osteotropic cells. Moreover, conditioned medium from EMMPRIN-overexpressing MDA-231 cells exhibited a significant increase of endothelial cell chemotactic activity, whereas conditioned medium from EMMPRIN-silenced cells prevented HUVEC cord-like formation. These results highlight the biological effects exerted by EMMPRIN-induced VEGF. In this regard, it has been previously shown that EMMPRIN is capable to stimulate tumor angiogenesis both *in vitro* and *in vivo* through upregulation of VEGF and MMP-9 in tumor and stromal compartments (11).

Bone is the most common site for metastasis in advanced breast cancer patients (35). There is evidence indicating that bone destruction at sites of osteolytic metastases is the result of osteoclast activity rather than of tumor cells per se (35, 36).

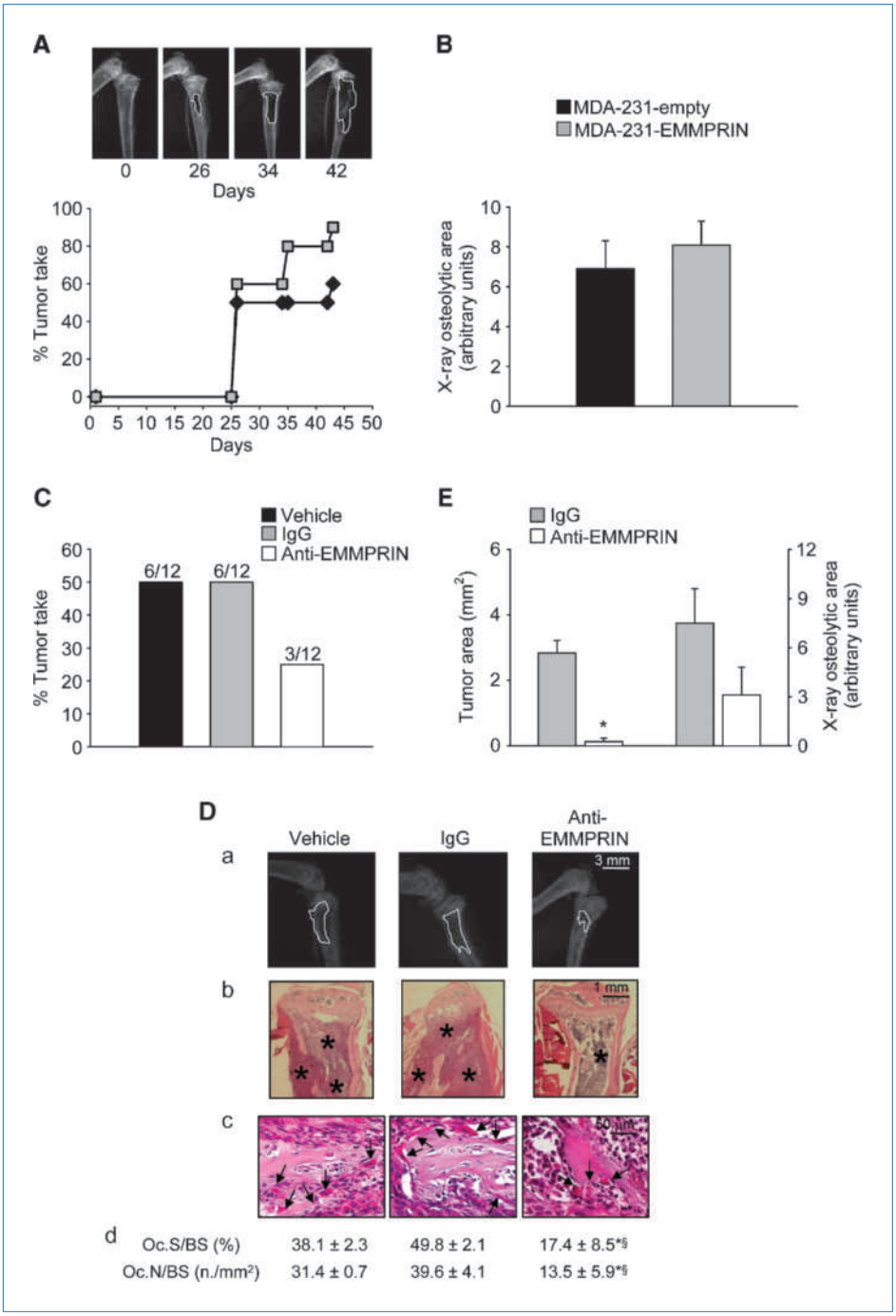

Figure 3. Intratibial injection of tumor cells. A and B, 4-wk-old female BALB/c-*nu*/*nu* mice were subjected to intratibial injection with a suspension (1×10^4 cells/10 μL PBS) of MDA-231-empty or MDA-231-EMMPRIN cells. A, evaluation of the incidence of tumor take evidenced as osteolytic lesions (gray square, MDA-231-empty; black square, MDA-231-EMMPRIN). Insets, X-rays of the hind limb of a mouse injected with MDA-231 cells taken at 26, 34, and 42 d after injection (solid line, osteolytic area). B, bone densitometric analysis of the radiographs assessing the osteolytic areas taken at the end point of the experiment. C to E, 4-wk-old BALB/c-*nu*/*nu* mice were subjected to intratibial injection with a suspension of MDA-231 cells. The day after injection, animals were treated with vehicle, 5 μg IgG1 control immune serum (IgG), or 5 μg EMMPRIN blocking antibody (anti-EMMPRIN), twice weekly until the end of the experiment. C, evaluation of the incidence of osteolytic lesions at the end point of the experiment (inset numbers, number of tibiae developing osteolytic lesions/number of tibiae injected). D, shown are (a) X-ray analysis (solid line, osteolytic areas) and (b and c) histologic analysis of one representative tibia for each group. b and c, H&E staining of tibia sections (*, tumor mass; arrows, osteoclasts). d, histomorphometric analysis of tibia sections (Oc.S/BS, osteoclast surface/bone surface; Oc.N/BS, osteoclast number/bs). For osteoclast surface/bone surface, $P = 0.014$ versus IgG (*) and $P = 0.049$ versus vehicle (§); for osteoclast number/bs $P = 0.013$ versus IgG (*) and $P = 0.028$ versus vehicle (§). Data are representative of two experiments. E, quantification of tumor area from histologic sections stained with H&E (left) and of the osteolytic lesions by densitometric analysis of radiographs (right). *, $P = 0.001$ versus IgG.

Indeed, tumor cells that colonize the bone produce factors that directly or indirectly promote the formation and activity of osteoclasts. Destruction of the bone matrix by osteoclasts results, in turn, in the release of tumor-seeking factors therein stored that further stimulate tumor spread (35–37). This reciprocal regulation between tumor cells and the bone microenvironment results in a vicious cycle that progressively increases both bone destruction and tumor burden (Fig. 6).

Our results indicated that overexpression of EMMPRIN increased the incidence of osteolytic lesions induced *in vivo* by intratibial injection of tumor cells. To the best of our knowledge, this is the first evidence indicating a role for EMMPRIN in tumor-induced osteolysis. Among the factors produced by tumor cells in the bone microenvironment, there is the parathyroid hormone/parathyroid hormone–related peptide, which in turn stimulates the production of RANKL in osteoblasts. RANKL is a key pro-osteoclastogenesis cytokine that acts on osteoclast precursors by binding with a membrane receptor termed RANK. The interaction between RANKL and RANK stimulates osteoclastogenesis and bone resorption by activating the NF-κB pathway (38). Herein, we have shown a link between tumor EMMPRIN and the RANKL pathway because treatment of MDA-231 cells with recombinant RANKL significantly increased EMMPRIN expression, MMP-9 mRNA and activity, and VEGF expression. We also showed that the increase in MMP-9 and VEGF induced by RANKL was EMMPRIN dependent because it was abolished after EMMPRIN knockdown by siRNA. Of note, RANKL produced by stromal-like tumor cells has been shown to enhance the expression of EMMPRIN mRNA in macrophage-like RAW264.7 cells during their differentiation into osteoclasts (39). In this study, we report a previously unrecognized interrelationship between the RANKL pathway and EMMPRIN expression in osteotropic breast cancer cells.

RANKL is primarily produced by osteoblasts as a cell surface protein that may be subjected to shedding by enzymatic cleavage. Increased RANKL expression by osteoblasts is a hallmark of bone metastases and is deemed to contribute to enhanced osteoclast activity at sites of osteolytic lesions (35). It is conceivable though that osteoblasts also contribute to tumor cell metabolism through the RANKL pathway, and indeed, conditioned medium from primary osteoblasts enhanced EMMPRIN protein expression in MDA-231 cells. Our data suggest that the mechanism whereby EMMPRIN induces osteolysis relies to a direct EMMPRIN activity as well as to the induction of the release of downstream effectors,

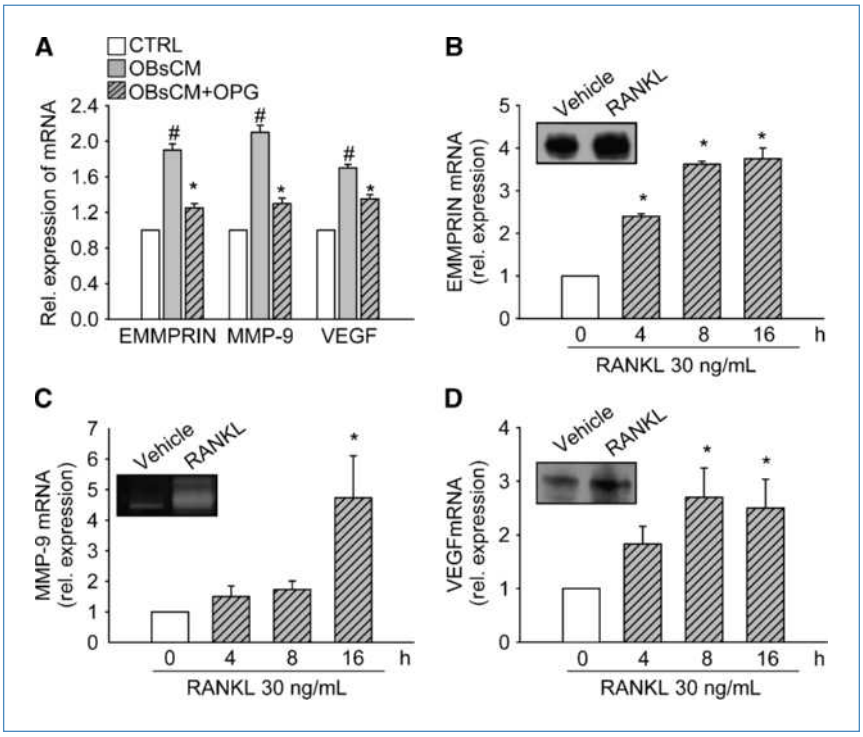

Figure 4. Effect of RANKL on the expression of EMMPRIN and its downstream genes. A, MDA-231 cells were treated with DMEM (CTRL) or with conditioned medium from primary mouse osteoblast cultures treated with vehicle (OBsCM) or 100 ng/mL OPG (OBsCM+OPG) for 48 h. The cells were collected, and the extracted RNA was reverse transcribed. The resulting cDNA was subjected to comparative real-time PCR using primer pairs and conditions specific for EMMPRIN, MMP-9, and VEGF. Data are normalized versus the housekeeping gene GAPDH. Columns, mean of three independent experiments; bar, SEM. *, $P < 0.05$ versus OBsCM; #, $P < 0.05$ versus CTRL. B-D, MDA-231 cells were treated with 30 ng/mL RANKL for 4, 8, and 16 h. Cells were collected, and the extracted RNA was reverse transcribed. The resulting cDNA was subjected to comparative real-time PCR using primer pairs and conditions specific for (B) EMMPRIN, (C) MMP-9, and (D) VEGF. Data are normalized versus the housekeeping gene GAPDH. Columns, mean of three independent experiments; bars, SEM. *, $P < 0.05$ versus vehicle. Inset, (B) protein expression of EMMPRIN, (C) MMP-9 activity in conditioned media, and (D) VEGF protein expression 16 h after RANKL administration, and are representative of three experiments with similar results.

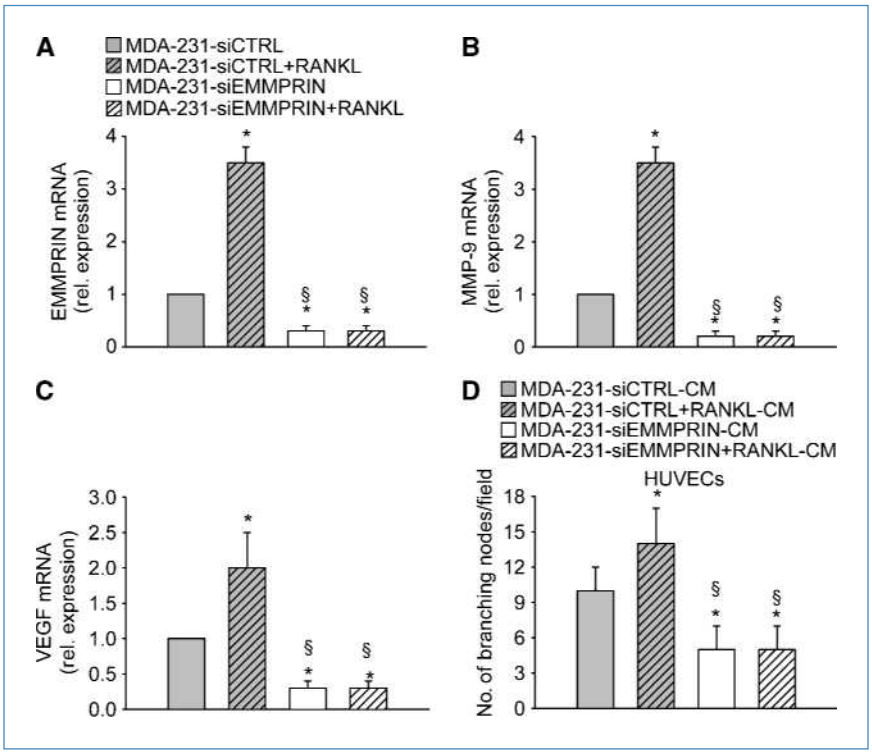

Figure 5. Effect of EMMPRIN knockdown on RANKL modulation. A to C, MDA-231 cells were subjected to RNA silencing using EMMPRIN-specific siRNA (MDA-231-siEMMPRIN) or scramble siRNA (MDA-231-siCTRL) as control for 48 h. Cells were subsequently treated with vehicle or 30 ng/mL RANKL for 16 h. RNA was then extracted and reverse transcribed. The resulting cDNA was subjected to comparative real-time PCR using primer pairs and conditions specific for (A) EMMPRIN, (B) MMP-9, and (C) VEGF. D, HUVECs were treated with conditioned media from MDA-231 silenced for EMMPRIN or scramble siRNA, and treated with vehicle or with 30 ng/mL RANKL. Average numbers of branching points were counted from triplicate wells. Columns, mean of three independent experiments; bars, SEM. *, $P < 0.05$ versus MDA-231-siCTRL; §, $P < 0.05$ versus MDA-231-siCTRL+RANKL.

including VEGF and MMP-9 (Fig. 6). MMP-9 is a MMP highly expressed in osteoclasts and is likely to act as collagenolytic enzyme during bone matrix degradation (38, 40). Of note, VEGF and MMP-9, together with bone resorption markers, were found to be positively correlated with bone metastases in patients with breast carcinomas (41). VEGF is known to directly enhance bone resorption and survival of mature rabbit osteoclasts (42). In keeping with these data, Aldridge and colleagues (43) reported that VEGF and RANKL together induced the differentiation of monocyte precursors into osteoclasts and bone resorption *in vitro*. It is thus feasible to hypothesize that local production of VEGF at the sites of bone metastasis may directly contribute to the formation of osteolytic lesions.

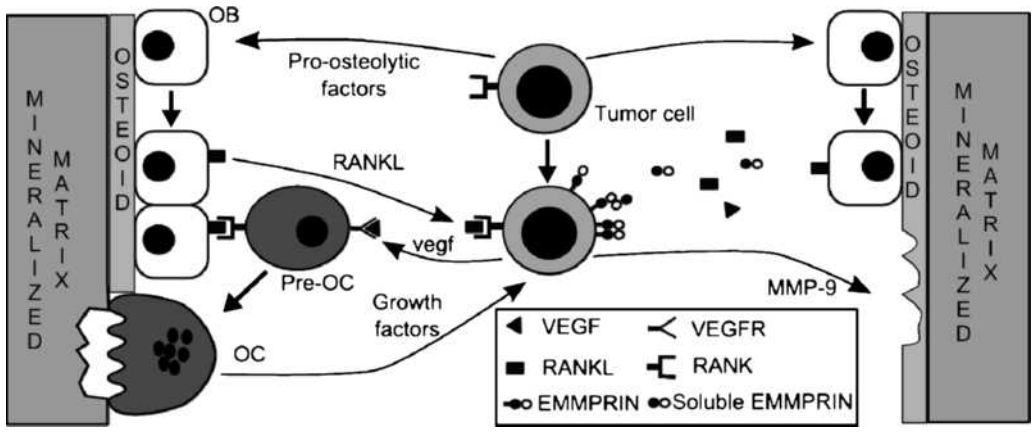

Figure 6. Schematic representation of the role played by EMMPRIN in the mechanism inducing osteolytic metastases. Molecular interactions among osteoblasts, osteoclasts, and tumor cells are shown. Tumor cells localized in the bone marrow produce factors (i.e., pro-osteolytic factors) that stimulate osteoclast formation by increasing the expression of RANKL on osteoblasts. RANKL binds to its receptor RANK and stimulates EMMPRIN expression in tumor cells. This in turn promotes the release of MMP-9 and VEGF. MMP-9 contributes to the digestion of organic matrix, whereas VEGF stimulates osteoclastogenesis. These two events favor tumor cells proliferation providing growth factors to tumor cells, thus contributing to the creation of the vicious cycle (Pre-OC, preosteoclast; OC, osteoclast; OB, osteoblast).

In conclusion, our findings show that EMMPRIN enhances the ability of human breast cancer cells to induce osteolytic lesions in mouse tibiae. The RANKL/RANK pathway mediates this effect and acts as one of the key players in the vicious cycle inducing the development of osteolytic bone metastasis (Fig. 6). These results not only emphasize the crucial role of EMMPRIN in tumor progression and in the formation of metastases, but also show the involvement of this molecule in breast cancer ability to grow into the bone. Our findings also provide evidence that EMMPRIN could be an alternative target for bone metastasis therapy, also in combination with anti-RANKL treatment.

Disclosure of Potential Conflicts of Interest

No potential conflicts of interest were disclosed.

Acknowledgments

We thank Dr. S. Zucker (Veterans Affairs Medical Center, Northport, NY) for providing the CD147-pcDNA3 plasmid and Dr. S. Constant (Department of Microbiology, Immunology and Tropical Medicine, the George Washington University, Washington, DC) for her kind support for the assessment of *in vivo* treatment with EMMPRIN blocking antibody.

Grant Support

European Commission grant METABRE (#LSHM-CT-2003-503049) and by a grant from the "Associazione Italiana per la Ricerca sul Cancro" (AIRC; A. Teti), and by a grant from AIRC (A. Angelucci).

The costs of publication of this article were defrayed in part by the payment of page charges. This article must therefore be hereby marked *advertisement* in accordance with 18 U.S.C. Section 1734 solely to indicate this fact.

Received 07/27/2009; revised 05/02/2010; accepted 05/25/2010; published OnlineFirst 07/14/2010.

References

1. Biswas C, Zhang Y, DeCastro R, et al. The human tumor cell-derived collagenases stimulatory factor (renamed EMMPRIN) is a member of the immunoglobulin superfamily. Cancer Res 1995;55:434–9.
2. Suzuki S, Sato M, Senoo H, Ishikawa K. Direct cell-cell interaction enhances pro-MMP2 production and activation in co-colture of laryngeal cancer cells and fibroblasts: involvement of EMMPRIN and MT1-MMP. Exp Cell Res 2004;293:259–66.
3. DeCastro R, Zhang Y, Guo H, et al. Human keratinocytes express EMMPRIN, an extracellular matrix metalloproteinase-inducer. J Invest Dermatol 1996;106:1260–5.
4. Marmorstein AD, Bonhila VL, Chiflet S, Neilla JM, Rodriguez-Boulan E. The polarity of the plasma membrane protein RETPE2 in the retinal pigment epithelium is developmentally regulated. J Cell Sci 1996;109:3025–34.
5. Finneman SC, Marmostein AD, Neill JM, Rodriguez-Boulan E. Identification of the retinal pigment epithelium protein RET-PE2 as CE-9/OX-47, a member of the immunoglobulin superfamily. Invest Ophthalmol Vis Sci 1997;38:2366–74.
6. Yan L, Zucker S, Toole BP. Role of the multifunctional glycoprotein, emmprin (basigin, CD147), in tumour progression. Thromb Haemost 2005;93:199–204.
7. Reimers N, Zafrakas K, Assmann V, et al. Expression of extracellular matrix metalloproteases inducer on micrometastatic and primary mammary carcinoma cells. Clin Cancer Res 2004;10:3422–8.
8. Gabison EE, Hoang-Xuan T, Mauviel A, Menashi S. EMMPRIN/CD147, an MMP modulator in cancer, development and tissue repair. Biochimie 2005;87:3861–6.
9. Caudroy S, Polette M, Nawrocki-Raby B, et al. EMMPRIN-mediated MMP regulation in tumor and endothelial cells. Clin Exp Metastasis 2002;19:697–702.
10. Sun J, Hemler ME. Regulation of MMP-1 and MMP-2 production through CD147/extracellular matrix metalloproteinase inducer interactions. Cancer Res 2001;61:2276–81.
11. Tang Y, Nakada MT, Kesavan P, et al. Extracellular matrix metalloproteinase inducer stimulates tumor angiogenesis by elevating vascular endothelial cell growth factor and matrix metalloproteinases. Cancer Res 2005;65:3193–9.
12. Millimaggi D, Mari M, D'Ascenzo S, Giusti I, Pavan A, Dolo E. Vasculogenic mimicry of human ovarian cancer cells: role of CD147. Int J Cancer 2009;35:1423–8.
13. Coleman RE. Clinical features of metastatic bone disease and risk of skeletal morbidity. Clin Cancer Res 2006;12:6243–9s.
14. Esteve FR, Roodman GD. Pathophysiology of myeloma bone disease. Best Pract Res Clin Haematol 2007;20:613–24.
15. Engel J, Eckel R, Kerr J, et al. The process of metastatisation for breast cancer. Eur J Cancer 2003;39:1794–806.
16. Clezardin P, Teti A. Bone metastasis: pathogenesis and therapeutic implications. Clin Exp Metastasis 2007;24:599–608.
17. Kingsley LA, Fournier PG, Chirgwin JM, Guise TA. Molecular biology of bone metastasis. Mol Cancer Ther 2007;6:2609–17.
18. Siclari VA, Guise TA, Chirgwin JM. Molecular interactions between breast cancer cells and the bone microenvironment drive skeletal metastases. Cancer Metastasis Rev 2006;25:621–33.
19. Crampton SP, Davis J, Hughes CC. Isolation of umbilical vein endothelial cells (HUVEC). J Vis Exp 2007;3:183.
20. Zucker S, Hymowitz M, Rollo EE, et al. Tumorigenic potential of extracellular matrix metalloproteinase inducer (EMMPRIN). Am J Pathol 2001;158:1921–8.
21. Marzia M, Sims NA, Voit S, et al. Decreased c-src expression enhances osteoblast differentiation and bone formation. J Cell Biol 2000;151:311–20.
22. Angelucci A, Gravina GL, Rucci N, et al. Evaluation of metastatic potential in prostate carcinoma: an *in vivo* model. Int J Oncol 2004;25:1713–20.
23. Rucci N, Recchia I, Angelucci A, et al. Inhibition of protein kinase c-Src reduces breast cancer metastases and increases survival in mice. J Pharmacol Exp Ther 2006;318:161–72.
24. Damsker JM, Okwumabua I, Pushkarsky T, Arora K, Bukrinsky MI, Constant SL. Targeting the chemotactic function of CD147 reduces collagen-induced arthritis. Immunology 2008;126:55–62.
25. Albini A, Iwamoto Y, Kleinman HK, et al. A rapid *in vitro* assay for quantitating the invasive potential of tumor cells. Cancer Res 1987;47:3239–45.
26. Muraoka K, Nabeshima K, Murayama T, Biswas C, Koono M. Enhanced expression of tumor-cell-derived collagenase-stimulatory factor in urothelium carcinomas: its useful as a tumor marker for bladder cancers. Int J Cancer 1993;55:19–26.
27. Polette M, Gilles C, Marchand V, et al. Tumor collagenase stimulatory factor (TCSF) expression and localization in human lung and breast cancers. J Histochem Cytochem 1997;45:703–7.
28. Van den Oord JJ, Paemen L, Opdenakker G, de Wolf-Peeters C. Expression of gelatinase B and the extracellular matrix metalloproteinase inducer EMMPRIN in benign and malignant pigment cell lesions of the skin. Am J Pathol 1997;151:665–70.
29. Caudroy S, Polette M, Tournier JM, et al. Expression of the extracellular matrix metalloproteinase inducer (EMMPRIN) and the matrix metalloproteinase-2 in bronchopulmonary and breast lesions. J Histochem Cytochem 1999;47:1575–80.
30. Yang JM, O'Neill P, Jin W, et al. Extracellular matrix metalloproteinase inducer (CD147) confers resistance of breast cancer cells to anoikis through inhibition of bim. J Biol Chem 2006;281:9719–27.
31. Zou W, Zhu H, Wu X. Inhibition of CD147 gene expression via RNA interference reduces tumor cell invasion, tumorigenicity and

increases chemosensitivity to paclitaxel in HO-8910pm cells. Cancer Lett 2006;248:211–8.
32. Li QQ, Wang WJ, Xu JD, Chen Q, Yang JM, Xu ZD. Up-regulation of CD147 and matrix metalloproteinase-2, -9 induced by P-glycoprotein substrates in multidrug resistant breast cancer cells. Cancer Sci 2007;98:1767–74.
33. Dean NR, Newman JR, Helman EE, et al. Anti-EMMPRIN monoclonal antibody as a novel agent for therapy of head and neck cancer. Clin Cancer Res 2009;15:4058–65.
34. Marieb EA, Zoltan-Jones A, Li R, et al. Emmprin promotes anchorage-independent growth in human mammary carcinoma cells by stimulating hyaluronan production. Cancer Res 2004;64:1229–32.
35. Roodman GD. Mechanisms of bone metastasis. N Eng J Med 2004; 350:1655–64.
36. Guise TA, Mohammad KS, Clines G, et al. Basic mechanisms responsible for osteolytic and osteoblastic bone metastases. Clin Cancer Res 2006;12:6213–6s.
37. Coleman RE. Metastatic bone disease: clinical features, pathophysiology and treatment strategies. Cancer Treat Rev 2001;27:165–76.
38. Teitelbaum SL, Ross FP. Genetic regulation of osteoclast development and function. Nat Rev Genet 2003;8:638–49.
39. Si AI, Huang L, Xu J, Kumta SM, Wood D, Zheng MH. Expression and localization of extracellular matrix metalloproteinase inducer in giant cell tumor of bone. J Cell Biochem 2003;89:1154–63.
40. Wucherpfennig AL, Li YP, Stetler-Stevenson WG, Rosenberg AE, Stashenko P. Expression of 92 kD type IV collagenase/gelatinase B in human osteoclasts. J Bone Miner Res 1994;9:549–56.
41. Voorzanger-Rousselot N, Juillet F, Mareau E, Zimmermann J, Kalebic T, Garnero P. Association of 12 serum biochemical markers of angiogenesis, tumour invasion and bone turnover with bone metastases from breast cancer: a cross sectional and longitudinal evaluation. Br J Cancer 2006;95:506–14.
42. Nakagawa M, Kaneda T, Arakawa T, et al. Vascular endothelial growth factor (VEGF) directly enhances osteoclastic bone resorption and survival of mature osteoclasts. FEBS Lett 2000;473:161–4.
43. Aldridge SE, Lennard TWJ, Williams JR, Birch MA. Vascular endothelial growth factor acts as an osteolytic factor in breast cancer metastases to bone. Br J Cancer 2005;92:1531–7.